

Watching molecules crowd: DNA double helices under osmotic stress

R. Podgornik¹, H.H. Strey, D.C. Rau, V.A. Parsegian^{*}

Laboratory of Structural Biology / DCRT and Division of Intramural Research / NIDDK, National Institutes of Health, Bethesda, MD 20892, USA

Abstract

Simultaneous measurements on the packing and energetics of high-density liquid crystalline DNA phases show that the crowding of long DNA polyelectrolytes at ever increasing concentrations is accomplished through straightening of the random coils that the double helix assumes in dilute solution. X-ray scattering by ordered phases reveals that the local straightening of the molecules is also accompanied by their progressive immobilization and confinement within the molecular 'cages' created by neighboring molecules. These effects can be clearly observed through the measured energies of DNA packing under osmotic stress and through the changes in structural and dynamic characteristics of X-ray scattering from DNA in ordered arrays at different concentrations. The character of the confinement of large DNA motions for a wide range of DNA concentrations is dominated by the soft potentials of direct interaction. We do not see the power-law variation of energy vs. volume expected from space-filling fluctuations of molecules that enjoy no interaction except the hard clash of steric repulsion. Rather, in highly concentrated DNA mesophases we see a crowding of molecules through electrostatic or hydration repulsion that confines their movements and positions. This view is based on directly measured packing energies as well as on concurrently measured structural parameters while the DNA double helices are condensed under an externally applied osmotic pressure.

Keywords: DNA; Osmotic stress; Molecular crowding; X-ray scattering

1. Introduction

In broadest terms 'macromolecular crowding' has come to designate conditions that lead to properties not seen in solutions so dilute as to be devoid of macromolecular interaction. Already several decades ago it was found that rod-like Tobacco Mosaic Virus particles formed concentrated birefringent phases that

fell out of solutions whose volume concentrations were only a few percent [1]. In 1949 Onsager showed [12] that even at such dilutions macromolecular collisions so lowered the orientational entropy of viruses in solution that it was favorable for the free energy of the whole preparation to concentrate most of the particles into an ordered, condensed phase of parallel particles in order to preserve the dilute condition of those that remained dissolved in isotropic freedom. Since that time ordered arrangements of macromolecules have been an important source of information about 'crowding' [24].

^{*} Corresponding author.

¹ On leave from J. Stefan Institute, Ljubljana, Slovenia.

Table 1

Persistence lengths l_p of various polymers in different solvents. DNA with its persistence length of 500–600 Å falls somewhere in the middle between the very flexible and the very stiff polymers. Data taken from Ref. [6]

Polymer	Solvent	l_p (nm)
Schizophyllan	Water	200
Xanthan	0.1 M NaCl	120
DNA	0.2 M NaCl	58–68
Poly(hexyl isocyanate)	Hexane	42
Poly(hexyl isocyanate)	Toluene	37
Cellulose trinitrate	Acetone	17
Poly(terephthalamide- <i>p</i> -benzohydrazide)	DMSO	11
Hyaluronic acid	Water	1

Our purpose in this essay is, first, to describe one strategy, Osmotic Stress, that makes it possible to measure not only changes in the arrangement of crowded molecules but also to measure the work needed to effect those changes. For several years this technique has been used to determine forces between macromolecules or between bilayer membranes [13]. Now we use it to see how these large soluble molecules resist ordering under crowded conditions.

Our second purpose is then to present results and lessons learned from one molecule, double helical DNA in several different ionic solutions.

Flexible enough to show random behavior, stiff enough to show rod-like character, DNA is an ideal model polymer to study the phase behavior of semi-flexible polymer solutions. Its intrinsic stiffness, expressed as a persistence length l_p measured in dilute solution, falls between that of very flexible (bio)polymers, such as hyaluronic acid, and very stiff ones, such as schizophyllan (Table 1). Due to its intrinsic stiffness, at high enough concentrations DNA forms ordered liquid crystalline phases [10]. DNA is also a strong polyelectrolyte with two unit charges per base pair, which makes it feasible to study the influence of electrostatic repulsion on the phase diagram by varying the ionic strength [7].

Since all DNA–DNA interactions in aqueous monovalent salt solutions are repulsive [15,18], one must always do work in order to concentrate DNA solutions. At small interhelical spacings there are exponentially decaying hydration forces [18], which seem associated with the energetic cost of removing bound water from molecular surfaces. Additionally

an electrostatic repulsion is expected which, like hydration repulsion, would vary approximately exponentially with a decay length equal to the Debye length of the solution, $\lambda_D = 3 \text{ \AA} / \sqrt{I}$ where I is the molar ionic strength [15]. Besides working against pure intermolecular repulsion, the system itself gradually loses more and more degrees of freedom through suppression of conformational fluctuations. As long as there is no sudden change in symmetry of the sample, these entropic contributions to the free energy can be described as effective or ‘renormalized’ forces. As used here the term ‘renormalized’ [16] refers mostly to the effect of the conformational fluctuations of long polymers in a condensed array that modifies the characteristic decay length of the underlying bare force, but does not modify its exponential character.

When one realizes that although the local configuration of a DNA molecule has been well understood since the early fifties, it is surprising that we still have only preliminary ideas regarding the energetics associated with DNA compaction. Although several phases have been observed in gravimetric mixtures of DNA, salt, and water and some packing geometries or structures proposed [10,19], the thermodynamics of these phases is only now being elucidated [15,18]. There may well be many reasons for this obvious discrepancy, but a major one is that it has not been clear how to measure the thermodynamic parameters of concentrated polymers, i.e., how to measure the activity coefficients (or, equivalently, the osmotic coefficients) of polyelectrolytes in very concentrated solutions (osmotic pressures exceeding 1 atm). In the case of DNA, the concentrated regime extends all the way to 800–900 mg/ml making the usual methodology (ultracentrifugation and optical densitometry [23]) for measuring activities of concentrated macromolecular solutions not applicable.

One of the earliest measurements of the thermodynamic work of DNA condensation was by Brian et al. [3]. Centrifugal force was used to concentrate DNA and optical spectroscopy used to measure DNA concentration. This method, however, is only practical for relatively low concentrations of DNA and, consequently, small applied forces (osmotic pressures less than ca. 7×10^5 dynes/cm²). We have been measuring the work to concentrate DNA by using applied osmotic stress [13]. Essentially, the

osmotic pressure of a concentrated DNA solution is set by equilibrating the DNA phase against a reservoir polymer solution (or vapor) of known water and small solute chemical potential. The concentration of the DNA phase is determined by X-ray scattering at very high externally imposed osmotic pressures or by direct densitometry at lower pressures and for less ordered DNA regimes. This method is especially well suited to study crowding of strongly interacting macromolecules such as DNA.

2. Method

The polymer used in the reference solution to set water, salt and small solute activities is usually polyethylene glycol (PEG), since DNA phase separates from solutions of fairly low concentrations of PEG, for example, about 8% PEG 8000 MW in 0.5 M NaCl. At lower concentrations of PEG or with polymers that do not phase separate from DNA, such as dextran, the separation of the reference polymer solution and the DNA phase must be enforced by a dialysis membrane (of the appropriate molecular weight cut-off). It is important that all other solutes such as salt, for example, be able to equilibrate between the stressing and DNA phases. The direct osmotic pressure experiment does require a precise knowledge of the osmotic stress generated by the osmotic agent (Osmotic pressure data for different polymers are obtainable on World Wide Web: <http://abulafia.mgsl.dcert.nih.gov/start.html>). Fortunately, ample measurements and calibrations have accumulated through the years such that osmotic stress experiments are now easily and accurately performed [13].

The general idea of an osmotic stress experiment is quite simple (Fig. 1). A stressing agent in vast volume excess at a known osmotic pressure and salt activity is equilibrated with DNA solution until thermodynamic equilibrium is reached. The equilibrium state of the combined (DNA and reference polymer solution) system is thus determined essentially through the chemical potentials of the stressing solutions. The equilibrium state corresponds either to an ordered DNA subphase, in which case X-ray scattering can be used to estimate its density, or to an isotropic DNA phase that yields to standard density

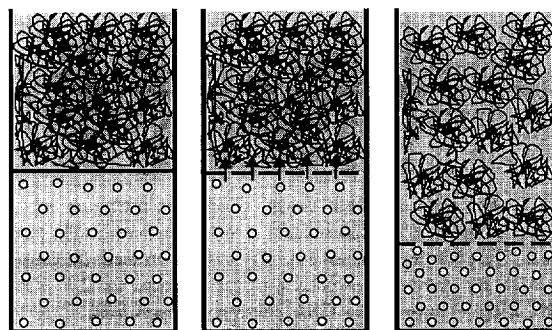


Fig. 1. The establishment of thermodynamic equilibrium between the stressing solution and the DNA subphase. After equilibrium is reached, the chemical potentials of all the permeating species (water, small ions) are equal. From left to right: (left) two solutions, DNA (bottom) and PEG, at arbitrary concentrations, separated by an impermeable barrier; (middle) the barrier is made semi-permeable and movable so that water and small solutes can pass in the direction of the solution with higher osmotic pressure; (right) osmotic equilibrium between two solutions where the upper 'stressing' solution reaches a concentration whose osmotic pressure can be independently measured and calibrated. Usually in practice this upper solution is in effectively infinite volume excess so as to act as a reservoir whose properties do not change during equilibration with the lower solution of ordered molecules.

measurement (e.g. gravimetric, optical absorption). The experiment is thermodynamically equivalent to applying pressure on the DNA phase with a semipermeable piston that allows water and salt to pass freely but not DNA [9]. The applied mechanical pressure is equivalent to the reference polymer solution osmotic pressure.

In contrast to experiments with gravimetric mixtures of DNA, salt, and water [10], the osmotic stress technique gives thermodynamic information because the activities of water and of all the small molecules in the stressing solution that are in equilibrium with the DNA phase are known. Changes in the DNA chemical potential with changes in the activities of water or salt in the stressing solution are related by a Gibbs–Duhem relation through the number of water molecules or salt ions associated with the DNA phase.

A note on terminology. We use the expression 'osmotic stress' whenever we refer to a *preset, calibrated* osmotic pressure of the PEG or dextran solution. We use the more general term 'osmotic pressure' in all the other cases, as, e.g., when referring to the osmotic pressure of DNA.

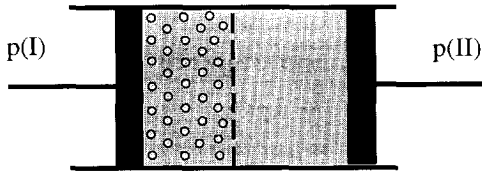


Fig. 2. The DNA + solvent phase (I) and the reference solvent (water) solution (II) in equilibrium across a semipermeable membrane. The pressure in phase I is $p(I)$ and the pressure in phase II is $p(II)$. By definition osmotic pressure is equal to $\Pi = p(I) - p(II)$. If the volume of the DNA phase is changed from V_1 to V_2 , so that $(V_1 - V_2)/v_w$ molecules are transported across the semipermeable membrane (v_w is the molecular volume of a single water molecule), the corresponding work is simply given by $\Pi(V_1 - V_2)$ for a small enough volume change. For finite volume change see main text.

Under conditions of constant salt activity and temperature, the osmotic pressure Π defines the rate of change of (Helmholtz) free energy F with exchangeable volume V ,

$$\left. \frac{\partial F}{\partial V} \right|_{T, \mu(\text{salt})} = -\Pi$$

The change in the free energy of the DNA phase ΔF as its volume decreases from V_1 to V_2 with increasing osmotic stress, Π , is

$$\Delta F = - \int_{V_1}^{V_2} \Pi(V) dV$$

It is obvious that this is the work done on the DNA phase by the piston (see Fig. 2) when the volume of

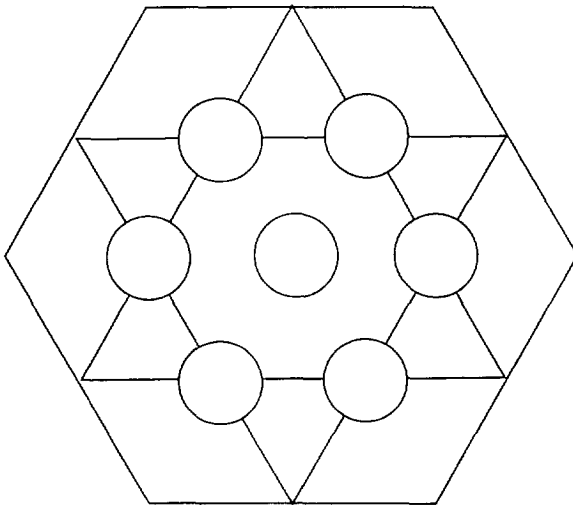


Fig. 3. A schematic representation of the high density DNA phase. The hexagonal symmetry and the small interhelical separation effectively immobilize the central molecule within a cage provided by its nearest neighbors. Left side: a view in the direction of the long axes of the molecules, right side: a view perpendicular to the direction of the long axes. The interhelical spacing corresponding to the picture on the r.h.s. is 25 Å (the scale of this picture corresponds to the real dimensions of DNA).

this phase is changed from V_1 to V_2 . It is completely analogous to the $-pdV$ work for an ordinary gas and it can be derived in the same way [4]. The integral above can be calculated by measuring the volume of the DNA phase at different values of the osmotic stress, Π , thus obtaining $\Pi(V)$.

3. Results

It is more convenient and pedagogically more illuminating to describe the *decrowding* of DNA as it proceeds from simple crystal-like order at tight packing to more complex arrays that allow molecular motion. This is crowding in reverse order, starting with DNA highly confined through direct or bare interactions with their neighbors, and gradually allowing the matrix to expand by lowering the external osmotic stress. As helices move apart and direct interactions weaken, the motions of helices increase, modifying the energetic scheme to include configurational entropies.

3.1. Regime of close packed DNA [18]

Here the effective interhelical spacing between the DNA molecules is relatively small, ca. 25-to-35 Å in NaCl, corresponding to ca. 5-to-15 Å separation between neighboring DNA surfaces.

In order to facilitate the conversion from the interhelical spacing to the concentration scale, we present conversion values in Table 2.

At even larger densities, with interaxial spacings less than about 24 Å, a structural transition from B- to A-form DNA occurs that is not connected with the direct comparison of B-DNA packing at lower densities. In the high density regime of B-DNA, X-ray scattering shows a microscopically ordered hexagonal columnar liquid crystal, with long range *positional* order in the plane perpendicular to the long axes of the molecules. The positional order in the direction parallel to the long molecular axes is quasi-crystalline at the highest density end of this regime and becomes liquid-like at the lower density end. It is not yet clear whether the range of the longitudinal order increases continuously or discontinuously with density in this regime. The *bond orientational order* [22] is definitely long range,

resulting in a diffraction pattern with hexagonal symmetry in X-rays scattered from a macroscopically oriented DNA array [17]. For short-fragment DNA the macroscopic orientation can be established by the imposition of a strong external magnetic field [2]. With long-fragment DNA the characteristic times involved with this ordering scheme are prohibitively large, and wet spinning [20] has proven a much more effective and practical way to create macroscopically ordered samples. The hexagonal *bond orientational order*, in contradistinction to the *positional order*, vanishes quite abruptly at the end of the high density regime, at $D_{\text{int}} \approx 32$ Å in 0.5 M NaCl [17].

Taking a look at the high density phase of DNA in the direction of the long axes of the DNA helices, one sees the following picture (see Fig. 3). The central molecule is caged within an hexagonal cell. At these high densities it is virtually impossible for the central polymer molecule to escape from the effective tube formed by its neighbors not only because of short range steric repulsion but more importantly because of long ranged, soft repulsive forces. The conformational fluctuations in the shape of the polymers are severely restricted by the interactions with neighbors. The energetics of packing is dominated by the bare (hydration) forces between the DNA helices which are exponentially decaying with the interhelical spacing [16]. The free energy per unit length, $f(D_{\text{int}})$, of the polymers in this density regime can be approximated as:

$$f(D_{\text{int}}) \sim f_0 e^{-D_{\text{int}}/\lambda_{\text{hyd}}}$$

where $\lambda_{\text{hyd}} \approx 3-4$ Å (see Ref. [16] for details). The molecules can thus be viewed as 'encaged' by their neighbors, preventing large conformational fluctuations, where the energetics of the phase is dominated by direct interactions between the molecules.

3.2. Regime of loosely packed DNA

At lower, osmotic stresses and larger interhelical spacings, beginning at 30 to 35 Å and continuing up to ca. 50 Å spacing (see Table 2 for the appropriate values of the DNA concentration), there are significant changes in the X-ray scattering pattern. Diffraction becomes diffuse and loses the hexagonal symmetry. Higher order diffraction becomes difficult and ultimately impossible to detect. For example, the left

Table 2

Connection between the concentration of DNA and the effective interhelical spacing assuming hexagonal symmetry of packing. The general connection between the concentration C in mg/ml and D_{int} in Å is: $C = (610/D_{\text{int}})^2$.

Interhelical spacing (Å)	Concentration (mg/ml)
20	930.25
30	413.44
40	232.56
50	148.84
60	103.36
70	75.94
80	58.14
90	45.94

diffraction pattern in Fig. 4 is from DNA equilibrated against 0.5 M NaCl and $\log_{10} \Pi$ [dynes/cm²] = 8 (ca. 100 atm). The interhelical spacing is 25.5 Å. The diffraction pattern on the right-hand side corresponds to 50.4 Å interhelical separation for DNA equilibrated against 0.5 M NaCl and $\log_{10} \Pi$ [dynes/cm²] = 6 (ca. 1 atm).

The increase in width of the first order equatorial

scattering peak is striking (see Fig. 4) and has been used to measure the corresponding increased motional disorder in the condensed DNA array [15]. The X-ray diffraction peak profile is Gaussian, a pattern that is consistent with each molecule of DNA moving in an effective external potential of cylindrical symmetry created by its neighbors. The shape of the diffraction peak also supports the view that the shape fluctuations of DNA are constrained mostly by the soft part of the interaction potential and not by its hard sterically colliding core. By quantifying the Gaussian shape of the diffraction peak in terms of the Gaussian fluctuation of the DNA molecule caged in a tube provided by its neighbors, one can directly deduce a value for the length of an independently fluctuating DNA unit as ≈ 40 –60 Å for the interaxial spacings 30–40 Å [14].

At the same time while the force vs. separation remains exponential, there is a doubling of the characteristic decay length compared with expected decay lengths. In salt solutions of greater than 1.0 molar concentration, the empirical decay length becomes $2\lambda_{\text{hyd}}$, while for lower concentrations the empirical decay length is twice the Debye length,

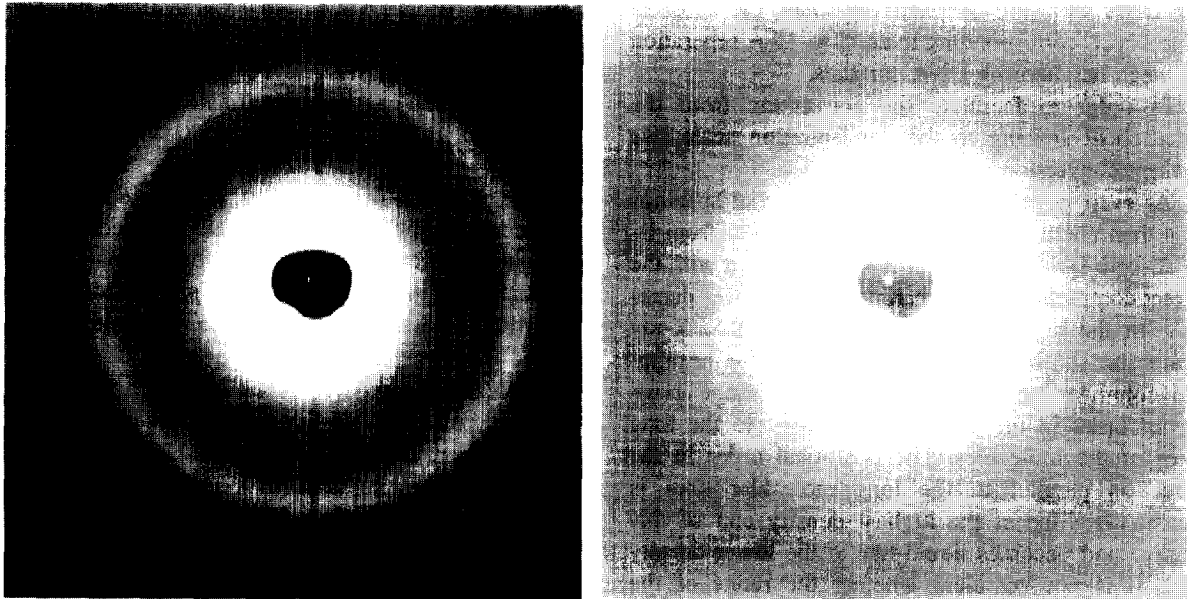


Fig. 4. X-ray diffraction patterns of condensed DNA subphase at two different values of osmotic stress, $\log \Pi$ [dynes/cm²] = 8 (left) and $\log \Pi$ [dynes/cm²] = 6 (right), both at 0.5 M NaCl salt. The broadening of the diffraction pattern is clearly visible and can be quantified through a model of positional disorder–shape fluctuations of the DNA molecules (see Ref. [15] for details).

$2\lambda_D$. Again this doubling, and perhaps eventual additional enhancement [21], of the λ_{hyd} and λ_D is due to the work being done to confine molecules under a centralizing force field created by its neighbors.

Beyond interaxial spacings ca. 55 Å, the loss of order is so great as to make it impossible to examine by X-ray diffraction. Solutions remain birefringent, and one can continue to measure the work of confinement under osmotic stress by measuring the DNA density directly by gravimetric methods.

4. Theory

The characteristic length describing the fluctuations of a polymer chain in a tube of effective diameter ca. 40–50 Å is obviously not the persistence length (ca. 500 Å for random sequence B-form DNA). Odijk [11] presented plausible arguments to the effect that the characteristic length imposed on a single DNA molecule in this phase is the deflection length, l_D , which can be orders of magnitude smaller than the bulk persistence length (see Fig. 5). For isolated polymer molecules the persistence length is defined in terms of the contour length along which polymer orientations are correlated or persist [5]. The deflection length is defined similarly, except that the memory of the initial configuration persists for a shorter length since a helix must change direction whenever it collides with its neighbors.

A simple energy argument [11] allows one to derive the following dependence of the deflection

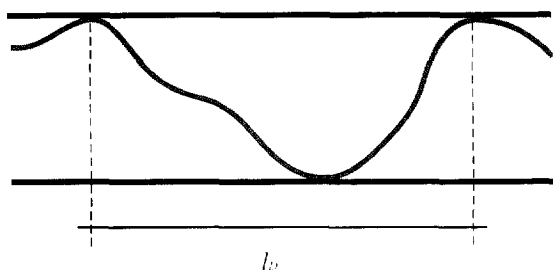


Fig. 5. Schematic picture of a polymer confined to a tube with diameter D . As soon as the polymer bumps into the wall it loses its orientational correlation. The deflection length l_D is a measure for the decay of this orientational correlation and is essentially given by the average distance between two bumps.

length l_D on the persistence length l_p and effective interhelical spacing $D_{\text{eff}} = D_{\text{int}} - D_0$

$$l_D \sim (l_p D_{\text{eff}}^2)^{1/3}$$

With the appropriate values of D_{int} and DNA diameter D_0 in this regime of DNA densities, we obtain an estimate ca. 50 Å. While Odijk's result is for molecules in a tube of diameter D_{eff} for molecules feeling no central force other than hard collisions with the walls, this result is only qualitatively relevant to the experimental situation [14]. Nevertheless it nicely shows that the correlation length will be much less than the persistence length because the tube or cage of dimension D_{eff} is so much less than l_p .

The additional degrees of freedom available to the polymers in the low density regime lead to modified energetics of the system. Although the energetics of the DNA condensed in the high density regime is dominated by direct, short range hydration repulsion (exponentially varying with a ca. 3–4 Å decay length [18]), the energetics in the lower density regime is not directly associated with bare hydration or even electrostatic potentials. The experimentally observed repulsion in the 35–55 Å spacing regime decays apparently exponentially with interhelical separation, but with a salt concentration dependent decay length that is about *twice* the expected (Debye) decay length for double layer repulsion or for hydration forces at salt concentrations greater than 1 M.

We proposed a model [14], where the underlying electrostatic interaction of the Debye–Huckel type or hydration force (depending on the bulk salt concentration) is modified by conformational fluctuations due to the wandering in the direction perpendicular to the long axes of the molecules in an external soft potential provided by nearest neighbors. A simple analysis of this effect leads to experimentally verifiable predictions. If the bare interhelical potential per unit length in a certain regime of D_{int} equals $f(D_{\text{int}})$, then it is modified by conformational fluctuations to the form

$$f_{\text{eff}}(D) \approx \text{const.} \sqrt{f(D)} \quad (6)$$

where *const.* is a slowly varying function of D_{int} . Measurements of osmotic pressure, basically a derivative of $f(D)$ with respect to D , give strong

support to this mechanism of interaction ‘renormalization’. The doubling of the decay length from the underlying direct potentials is a straightforward consequence of the $\sqrt{f(D)}$ term. By converting the measured $f_{\text{eff}}(D)$ into the bare $f(D)$ we were also able to estimate the magnitude of the bare electrostatic interaction between the DNA helices that turned out to be pleasingly close to the value obtained from computations in frozen hexagonal arrays (K. Sharp, personal communication). At high salt, where the electrostatic interactions are effectively suppressed, the hydration part of the interaction is renormalized to

$$f_{\text{eff}}(D) \approx f_{0,\text{eff}} \times e^{-D_{\text{int}}/2\lambda_{\text{hyd}}}$$

The doubling of the direct interaction decay length can thus be viewed as a fingerprint of fluctuational degrees of freedom.

Concurrent with the fluctuational broadening of the first diffraction peak, we observe that hexagonal texture of the macroscopically ordered wet-spun samples and also that the second order diffraction peaks are gone.

Examination of the force curve over the entire 25–55 Å spacing regime shows that the transition

from the fluctuation enhanced potentials seen at large spacings to the direct repulsive forces is not gradual but quite abrupt, occurring at about 30–35 Å [16]. This change in the force character is also accompanied by a sudden change in the texture of the DNA samples seen under crossed polarizers, though the texture within each regime remains unchanged. In the large density, bare potential dominated regime, the texture corresponds to a columnar hexagonal liquid crystal, whereas in the low density, fluctuation dominated regime the texture is consistent with a cholesteric liquid crystal. Fig. 6 shows the texture of the two samples under crossed polarizers so that a progression from dark to illuminated portion of the sample presupposes a 90° change in the average director of the DNA molecules.

Although the onset of the fluctuational degrees of freedom of a single DNA molecule in its hexagonal cage appears quite abrupt, it corresponds either to a second order or to a weak first order phase transition as there is no or very little observable volume change at the transition osmotic pressure.

The implications of the different energetics of DNA in the hexagonal columnar and cholesteric phases are fundamental. As already stated, in the



Fig. 6. Texture of the DNA condensed subphase under crossed polarizers ($\times 100$). Right-side: texture just above the transition at about 30–35 Å (see main text for details); left-side: texture just after the transition showing the ‘fingerprint’ pattern characteristic of the cholesteric mesophase. The two textures correspond to hexagonal and cholesteric liquid crystals, respectively.

high density hexagonal columnar phase the most important are the bare short-range interactions. The dependence of the osmotic pressure in this phase on the DNA density clearly shows enough details in the interaction potential that it would be quite unrealistic to approximate it with a hard core repulsion. How important the soft structure of the short range potential is for the phase transition itself remains to be seen.

The dominant interactions in the cholesteric phase are fluctuationally ‘renormalized’ bare electrostatic interactions. The bare potentials are completely masked by the presence of strong configurational fluctuations. But then again the interactions can not be approximated just by fluctuation repulsion in an underlying hard core background potential. A soft potential does not allow fluctuating helices to fill the hexagonal space in the same way as simple hard sterics. Models for calculating entropic repulsions that assume this type of interaction are not consistent with the measured Gaussian-like character of the diffuse equatorial scattering peaks. The power law interactions based on an underlying hard core bare interaction potential simply cannot describe the entropic contributions from fluctuations of strongly interacting molecules. The interplay between interactions and fluctuations is quite intricate leading to a ‘renormalized’ bare potential rather than a pure fluctuation repulsion. The form of bare interhelical potentials thus appears to be crucial. Again it is difficult to assess at this point whether the detailed form of the potential is also important for the sequence of mesophases as the system is even further diluted.

At even smaller DNA densities, corresponding to effective interaxial separations greater than about 55 Å at 0.5 M uni–uni valent salt, new classes of motions are possible. DNA helices are now so loosely packed that it is energetically feasible for a polymer to escape from its hexagonal cage and move into an adjacent one. One can thus create ‘vacancies’ and ‘interstitials’ in dynamic equilibrium. The long range order in the plane perpendicular to the long axes of the molecules is obviously lost. Schematically, the migration of the DNA molecule from one hexagonal cage to the next one is illustrated in Fig. 7.

The characteristic longitudinal length scale for this class of motion is connected with the deflection length introduced previously. In addition, however,

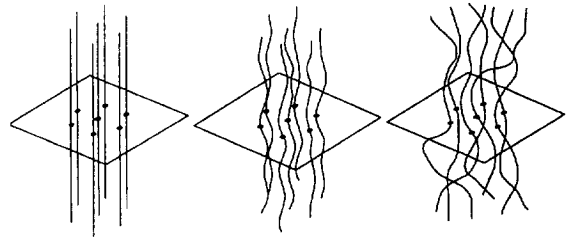


Fig. 7. Three regimes of configurational disorder in the condensed DNA phase. Left: at very high densities DNA molecules are effectively encaged by their neighbors, making conformational fluctuations impossible. Middle: at smaller densities the molecules are still encaged but are now permitted to exhibit conformational fluctuations within the molecular cages. Right: at still smaller densities, the DNA molecules can escape the cages and wander between them, creating ‘vacancies’ and ‘interstitials’.

to simply losing orientational correlation within a tube, the molecule must now also pass the energetic barrier associated with its hopping from one effective cage to the next one. A simple probabilistic argument can relate the ‘hopping length’ l_H to the Odijk deflection length

$$l_H \approx l_D \times e^{\Delta E/kT}$$

where ΔE is the maximum energy penalty for the polymer for getting from one cage to the next one. It should be on the order of the interaction energy of two skewed DNA rods at half the interhelical spacing [16].

Obviously this regime of DNA densities would correspond to very pronounced conformational fluctuations of the polymer chains that should modify the interhelical forces even further. Our initial experiments at very low osmotic stresses suggest that additional motions do come into play and that the qualitative character of the observed forces also consequently changes.

5. Perspective

Having established the ability to map the energy of formation onto the phase diagram of crowding molecules, one is struck almost as much by what is *not* seen as by what *is* seen.

The rigid ordering of molecules into a hexagonal structure at high density is to be expected among mutually repelling rod-like molecules. That the work

of pushing these molecules together in this regime should show their direct interaction seems a natural consequence. The sudden appearance of molecular motion is a puzzle; the transition to a cholesteric phase that allows this motion seems too smooth for the first-order transition that is expected on general symmetry grounds, but thus far undetected.

Once this motion begins, the work needed to confine it completely overwhelms the direct intermolecular forces that in fact enforce molecular order. It is more realistic to consider that the molecules move in a tube (or a cage) with a centralizing soft force rather than in a tube defined only through steric hard core repulsions with its neighbors. This is quite contrary to all expectations from earlier models of molecular confinement which were built on the idea that molecule moves freely until it suddenly encounters a repulsion so strong as to be considered an infinitely hard wall. Within the confines of such hard walls, molecules were expected to move freely, their configurational free energy a simple logarithmic function of the cross-sectional area or volume available to them, a generalization of the work needed to confine an ideal gas to its volume. Such geometric thinking always leads to the prediction that the force or pressure of confinement be a simple power of the molecular separation or of the available volume.

This is not seen (see Fig. 8). Instead, the work of confinement goes as an exponential whose characteristic length is twice that of the underlying, confining intermolecular force. The Gaussian distribution of molecular position and corresponding X-ray diffraction intensity compels one to realize that the molecules are always feeling the long-range forces that guide them.

As the molecules move along the tube of their neighbors, they try to deviate from the position of least repulsion, wander off a bit only then to be forced back away from their drift in such a way that each segment of ca. 50 Å moves essentially independently. The natural stiffness of the molecule, with its persistence length some ten times greater than this, is irrelevant here.

Further dilution brings greater motion, possibly also further enhancement of the underlying decay length of direct interhelical interaction, and possibly finally a power-law repulsion when separations are so large that molecular interactions are a kind of thin

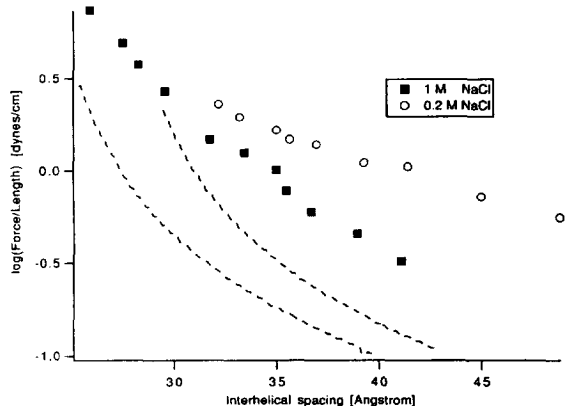


Fig. 8. The measured forces in an array of DNA helices are not of the fluctuation-steric repulsion type (dashed lines). They always show the detailed characteristics of the underlying soft (as opposed to the hard steric exclusion) interaction potential. The data points are for DNA in 1 (■) and 0.2 (○) M NaCl solutions. The theoretical curves have been obtained for hard steric exclusion modified by hydration (lower) or electrostatic repulsion (upper dashed curve). The theoretical curves obviously represent a different scaling class (from Ref. [14]).

skin that no longer pervades the full space in which molecules move [14,21].

This leads to still-uncharted territory. Should the breakdown of order be treated as an accumulation of defects in ordered structure? Is there a fragmentation of ordered regions into small domains? Should we begin to think of individual molecules with their random-walk configuration of dilute solution simply interfering with each other as their radii of gyration approach average intermolecular distances?

The energies associated with different conformations of highly concentrated polyelectrolyte solutions will be extracted using osmotic stress experiments. Far more complicated theories will be necessary to connect interaction potentials, structure and conformational disorder with these measured energies. Analogies with the configurations of magnetic vortex arrays (Abrikosov lattice) in superconducting materials might provide an unexpected source of ideas [8].

The crowding of strongly interacting molecules can be systematically addressed. It is possible to extract experimentally the relevant numerical parameters (deflection length, 'renormalized' decay lengths, amplitude of fluctuations etc.) that connect structure and thermodynamics and to go beyond the idealiza-

tion of effectively hard-walled molecules that have guided our thinking so far.

Acknowledgements

One of the authors (H.H.S.) thanks the Deutsche Forschungsgemeinschaft for a scholarship. We would like to thank R. Bruinsma, K. Merchant, D. Nelson, J. Prost, A. Rupperecht, T. Strzelecka for stimulating discussions and M. Hodoscek (LSB/MGSL/DCRT/NIH) for help with molecular graphics.

References

- [1] J.D. Bernal and I.J. Fankuchen, *Gen. Physiol.*, 25 (1941) 111.
- [2] R. Brandes and D.R. Kearns, *Biochemistry*, 25 (1986) 5890.
- [3] A.A. Brian, H.L. Frisch and L.S. Lerman, *Biopolymers*, 20 (1981) 1305.
- [4] J. des Cloizeaux and G. Jannink, *Polymers in Solution*, Clarendon Press, Oxford, 1990.
- [5] M. Doi and S.F. Edwards, *The Theory of Polymer Dynamics*, Oxford University Press, New York, 1986.
- [6] H.-G. Elias, *Macromolecules*, Plenum Press, New York, 1984.
- [7] M.D. Frank-Kamenetskii, V.V. Anshelevich and A.V. Lukashin, *Sov. Phys. Usp.*, 40 (1987) 317.
- [8] R.D. Kamien, P. Doussal and D.R. Nelson, *Phys. Rev. A*, 45 (1992) 8727.
- [9] S. Leikin, D.C. Rau and V.A. Parsegian, *Phys. Rev. A*, 44 (1991) 5272.
- [10] F.J. Livolant, *J. Mol. Biol.*, 218 (1991) 165.
- [11] T. Odijk, *Macromolecules*, 16 (1983) 1340.
- [12] L. Onsager, *Ann. N.Y. Acad. Sci.*, 51 (1949) 627.
- [13] V.A. Parsegian, R.P. Rand, N.L. Fuller and D.C. Rau, *Methods Enzymol.*, 127 (1986) 400.
- [14] R. Podgornik and V.A. Parsegian, *Macromolecules*, 23 (1990) 2265.
- [15] R. Podgornik, D.C. Rau and V.A. Parsegian, *Macromolecules*, 22 (1989) 1780.
- [16] R. Podgornik, D.C. Rau and V.A. Parsegian, *Biophys. J.*, 66 (1994) 962.
- [17] R. Podgornik, H.H. Strey, A. Rupperecht, D.C. Rau and V.A. Parsegian, *Biophys. J.*, 68 (1995) A336.
- [18] D.C. Rau, B.K. Lee and V.A. Parsegian, *Proc. Natl. Acad. Sci. USA*, 81 (1984) 2621.
- [19] R.L. Rill, T.E. Strzelecka, M.W. Davidson and D.H. Van Winkle, *Physica A*, 176 (1991) 87.
- [20] A. Rupperecht, *Acta Chem. Scand.*, 20 (1966) 494.
- [21] J.V. Selinger and R.F. Bruinsma, *Phys. Rev. A*, 43 (1991) 2922.
- [22] K.J. Strandburg, *Bond-Orientational Order in Condensed Matter Systems*, Springer Verlag, Berlin, 1991.
- [23] C. Tanford, *Physical Chemistry of Macromolecules*, John Wiley, New York, 1961.
- [24] S.B. Zimmerman and A.P. Minton, *Ann. Rev. Biophys. Biomol. Struct.*, 22 (1993) 27.